

Received:  
30 January 2022

Revised:  
21 March 2022

Accepted:  
24 March 2022

Published online:  
19 April 2022

<https://doi.org/10.1259/bjr.20220135>

Cite this article as:

Rutman AM, Wangaryattawanich P, Aksakal M, Mossa-Basha M. Incidental vascular findings on brain magnetic resonance angiography. *Br J Radiol* (2023) 10.1259/bjr.20220135.

## REVIEW ARTICLE

# Incidental vascular findings on brain magnetic resonance angiography

<sup>1,2</sup>AARON M RUTMAN, MD, <sup>2</sup>PATTANA WANGARYATTAWANICH, MD, <sup>2</sup>MEHMET AKSAKAL, MD and <sup>3</sup>MAHMUD MOSSA-BASHA, MD

<sup>1</sup>Department of Radiology, Washington Permanente Medical Group, Seattle, WA, United States

<sup>2</sup>Department of Radiology, University of Washington School of Medicine, Seattle, WA, United States

<sup>3</sup>Department of Radiology, University of North Carolina, Chapel Hill, NC, USA

Address correspondence to: Dr Aaron M Rutman

E-mail: [arutman@uw.edu](mailto:arutman@uw.edu)

### ABSTRACT

Given the ever-increasing utilization of magnetic resonance angiography, incidental vascular findings are increasingly discovered on exams performed for unconnected indications. Some incidental lesions represent pathology and require further intervention and surveillance, such as aneurysm, certain vascular malformations, and arterial stenoses or occlusions. Others are benign or represent normal anatomic variation, and may warrant description, but not further work-up. This review describes the most commonly encountered incidental findings on magnetic resonance angiography, their prevalence, clinical implications, and any available management recommendations.

### INTRODUCTION

Magnetic resonance angiography (MRA) of the head is performed for many indications, most commonly for transient ischemic attack or stroke assessment and evaluation for aneurysm or vascular malformation, and less frequently for inflammatory conditions, mass effect, and surgical planning. With increased availability, frequency of acquisition, and quality of MRA, there is increased likelihood of discovering incidental vascular findings. While unrelated to the purpose of acquisition, incidental findings represent unexpected observations of potential or unknown clinical significance. This introduces the question: what to do about a finding which may have no consequence acutely, but may or may not be clinically relevant in the future? Importantly, detection can be detrimental if it leads to unnecessary treatment or follow-up. Incidental findings can be separated into two categories: those needing surveillance and/or treatment, and benign lesions or anatomic variants that may warrant description but not further work-up. Accurately diagnosing incidental pathology aids the clinician in establishing a plan of treatment or surveillance. Likewise, understanding common benign and anatomic variants allows the patient to avoid unnecessary treatment and/or follow-up.

#### Time-of-flight MRA technique

MRA protocols are typically implemented with time-of-flight (TOF) technique, usually without intravenous

contrast (although contrast material may be used to mitigate flow, turbulence, and susceptibility artifacts). In TOF sequences, stationary tissues are magnetically saturated by multiple RF pulses, while blood rushing into the imaged volume (having not yet experienced the saturation pulses) retains high initial magnetization. Stationary tissues remain dark, while inflowing blood is bright—a phenomenon known as “flow-related enhancement”. Contrast between the bright flowing luminal contents and dark stationary tissues is ideal for the creation of maximum intensity projections, which aid in interpretation of the angiogram.

Pathologies affecting the luminal caliber (including stenosis, occlusion, and dilatation) are well appreciated on TOF sequences. Maximum enhancement occurs with high flow velocities and when the vessel is perpendicular to the plane of imaging. As such, “arterialized” flow-related enhancement can be seen in venous structures in the setting of arteriovenous shunting, while abnormal slow flow due to upstream stenosis may attenuate signal. Additionally, flow-related enhancement may be artifactually decreased in arteries parallel to the imaging plane, or more apparent in veins that are perpendicular to the imaging plane. Finally, note that turbulent flow with associated spin-dephasing may also result in artifactual signal loss which can be mistaken for luminal pathology. MRA is also particularly susceptible to motion artifacts relative to computed

tomographic angiography (CTA). While artifacts may not represent true incidental findings *per se*, it is important to recognize common MRA artifacts, and recommend repeat imaging or alternate modalities when appropriate.

## INCIDENTAL PATHOLOGY

### Aneurysm

Unruptured intracranial aneurysms are commonly discovered incidentally. The prevalence of unruptured aneurysm is approximately 2.8%, with higher prevalence among females, and with increasing age.<sup>1–4</sup> Intracranial aneurysms are focal pathologic arterial outpouchings. Most are found in the anterior circulation, usually at junctions or bifurcations, including at the anterior cerebral artery (ACA) and anterior communicating artery (ACoA) (~30%), terminal internal carotid artery (ICA) (~30%), and middle cerebral artery (MCA) (~25%) (Figure 1). Less common locations include the extradural ICA (<10%) and vertebrobasilar arteries (<10%).<sup>5</sup> Notably, multiple aneurysms are found in 15–30% of aneurysm patients,<sup>3</sup> emphasizing the importance of avoiding satisfaction of search errors after finding a single aneurysm.

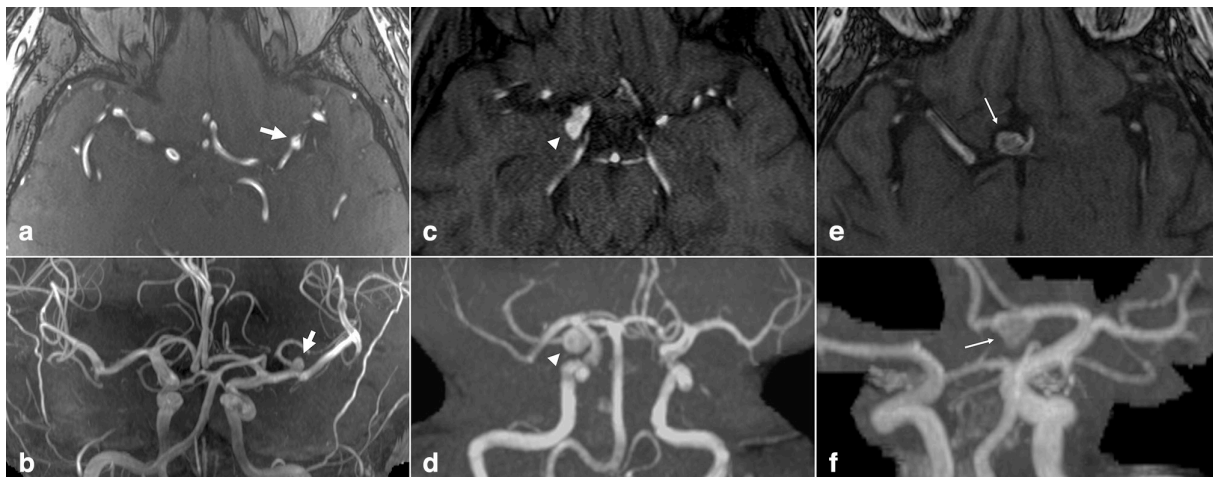
Prevalence of aneurysm increases in populations with specific modifiable, vasculopathic, and genetic risk factors.<sup>1,3,6,7</sup> Incidence is increased in those with a strong family history and certain genetic conditions including autosomal dominant polycystic kidney disease (ADPKD) and some connective tissue disorders. Although these syndromes increase risk (ADPKD increases risk 3–14-fold), they constitute <10% of patients with aneurysm.<sup>3,8</sup> The American College of Radiology considers MRA or CTA of the head appropriate for aneurysm screening in asymptomatic patients with ADPKD, previously treated or ruptured aneurysm, or those with  $\geq 2$  immediate family members with history of aneurysm.<sup>9</sup>

Sensitivity of MRA for intracranial aneurysm has been variously reported between 74 and 98%, with higher sensitivities for aneurysms > 3mm.<sup>10</sup> Sensitivity is improved with higher field-strength magnets; one 3T MRA-based study reported accuracies of 96–97% for small aneurysms  $\leq 5$ mm.<sup>11</sup> Pitfalls include difficulty differentiating from infundibulum, as small associated vessels may be poorly detected.

Given that subarachnoid hemorrhage carries high rates of morbidity and mortality (8–67%),<sup>4,12,13</sup> incidentally discovered aneurysm requires surveillance or treatment to monitor and mitigate risk of rupture. The proportion of growing aneurysms is approximately 3% per aneurysm-year, and higher growth rates are seen in aneurysms of larger size, non-saccular shape (14.7% per year), and involving the cavernous ICA (14.4% per year).<sup>14</sup> Interval growth is also an important risk factor for rupture (3.1% per year vs 0.1% per year for non-growing aneurysms).<sup>14</sup> Certain aneurysm morphologies are also associated with higher risk of rupture, including increased perpendicular height and higher size ratio (ratio of maximum diameter to parent vessel diameter).<sup>15</sup> Recent studies employing high-resolution vessel wall MR imaging (VWI) suggest a higher rupture risk in aneurysms with wall enhancement.<sup>16</sup>

Aneurysm location, size, and shape should be described to assist in risk stratification. Lifestyle modifications including smoking cessation and medical intervention can be implemented to lower rupture risk.<sup>3</sup> The optimal interval and duration of surveillance is not certain, but for unruptured aneurysms managed conservatively, a first follow-up at 6–12 months, followed by subsequent yearly or every-2-years follow-up is reasonable.<sup>3</sup> Small, low risk aneurysms which are stable on multiple follow-up studies can likely be surveilled more conservatively, while larger aneurysms with high-risk morphology and patient characteristics should be

Figure 1. Intracranial aneurysm. Axial TOF MRA (a) and 3D MIP reconstruction (b) demonstrate a 5 mm saccular aneurysm projecting superiorly from the left MCA bifurcation (arrows). Axial TOF MRA (c) and 3D MIP reconstruction (d) in a different patient demonstrate a 9 mm saccular aneurysm projecting posteriorly from the right PCoA origin (arrowheads). Axial TOF MRA (e) and 3D MIP reconstruction (f) in a different patient demonstrate a 10 mm saccular aneurysm projecting anterior/inferior from the right ACoA origin (small arrows). PCoA, posterior communicating artery; MIP, maximum intensity projection; MCA, middle cerebral artery; MRA, MR angiography; TOF, time-of-flight.



followed more closely. For those undergoing repeated follow-up, MRA rather than CTA can be considered to avoid frequent doses of ionizing radiation.<sup>3</sup> Further evaluation by VWI could be considered to confirm aneurysm stability.<sup>17</sup>

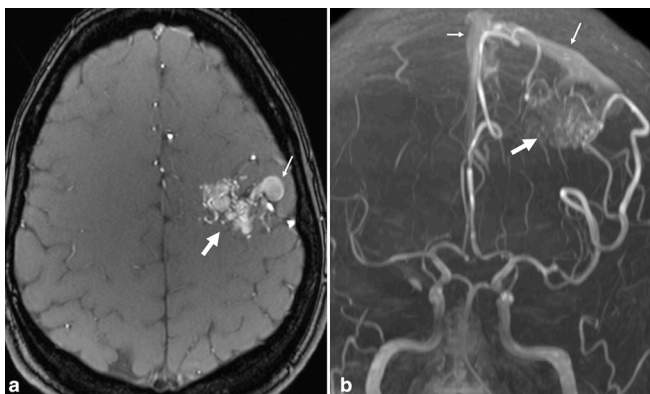
### Arteriovenous malformation

Brain arteriovenous malformations (AVM) are rare, seen in approximately 18 per 100,000 adults.<sup>18</sup> AVM may be incidental, symptomatic-but-unruptured, or ruptured. Approximately, two-thirds are discovered after symptomatic hemorrhage and one-fifth after seizure, but at least 15% are discovered incidentally in asymptomatic patients.<sup>18</sup> Although rare, AVM accounts for ~3% of stroke, ~4% of intracerebral hemorrhage, and ~9% of subarachnoid hemorrhage in young adults.<sup>18,19</sup> The largest risk factor for AVM hemorrhage is previous hemorrhage. Annual bleeding rate without previous hemorrhage is 1–6%,<sup>19–22</sup> and studies show modest increases in hemorrhage risk for larger AVMs, in deep anatomic locations, with deep/central venous drainage, and in pregnancy.<sup>20–22</sup>

It should be noted that the sensitivity of non-contrast TOF-MRA for detection of AVM is lower than that of CTA and conventional T2 weighted MRI. One study showed sensitivity for unruptured AVM of 71% for MRA, compared to 96% for CTA and 97% for T2 weighted MRI.<sup>23</sup> This may be due to unpredictable flow velocities and flow turbulence within AVMs, limiting visualization of a smaller nidus. MRA is also limited in depiction of draining veins. Associated aneurysms are also better detected by CTA, with a sensitivity of 88%, compared to 27% for MRA.<sup>23</sup>

On MRA, AVM is characterized by enlarged feeding arteries, a tangle of serpiginous vessels (representing the nidus), and irregular draining veins with flow-related enhancement due to shunting (Figure 2). Given the high morbidity and mortality associated with rupture, accurate diagnosis and further characterization with catheter-based digital subtraction angiography

Figure 2. Arteriovenous malformation. Axial TOF MRA (a) and 3D MIP reconstruction (b) demonstrate flow-related enhancement in a tangle of serpiginous vessels in the left posterior frontal lobe (large arrows). Early arterialized flow-related enhancement is seen in large, abnormal draining veins and in the superior sagittal sinus (small arrows), reflecting shunting. MIP, maximum intensity projection; MRA, MR angiography; TOF, time-of-flight.



(DSA) may be needed for appropriate treatment planning.<sup>24,25</sup> The Spetzler-Martin grading scale stratifies the surgical risk of resection,<sup>26</sup> grading AVMs based on lesion size, pattern of venous drainage (exclusively deep versus superficial), and neurological eloquence of adjacent brain. Higher grade AVMs are associated with increased rates of post-operative complications. As such, incidental AVM description should include size, location, and venous drainage; a description of arterial supply is also helpful for surgical and endovascular planning.

There is no consensus on the treatment of incidental AVM, as the morbidity and mortality of treatment may exceed that of untreated AVM's natural history.<sup>19,27</sup> However, as AVMs lack a capillary bed and do not supply normally functioning brain parenchyma, endovascular occlusion can often be performed without causing cerebral ischemia, making it a preferable treatment when feasible. Ultimately, management may be multimodal, including observation, microsurgical resection, endovascular embolization, and/or stereotactic radiosurgery.

### Dural arteriovenous fistula

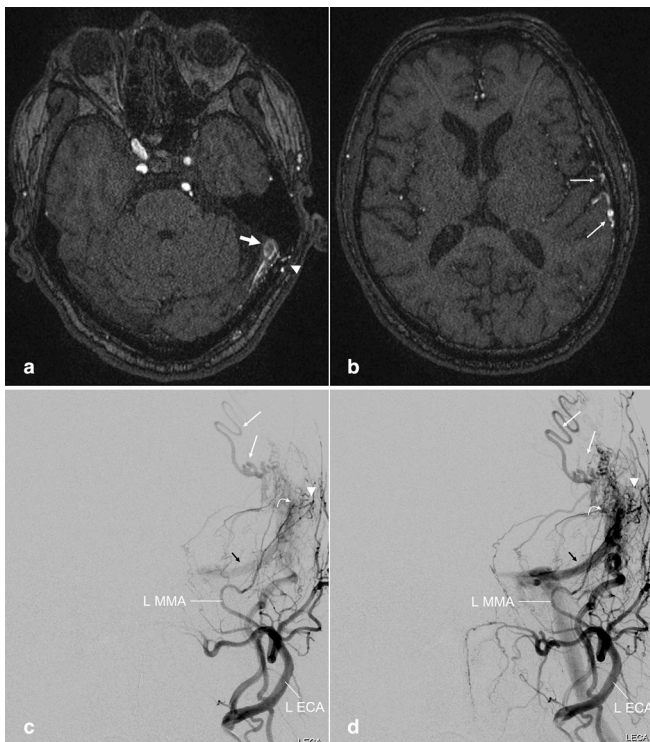
Dural arteriovenous fistula (dAVF) is a rare but distinct subtype of vascular malformation, accounting for approximately 10–15% of intracranial AVMs.<sup>28</sup> True prevalence is unknown. While traditional AVMs are generally surrounded by brain parenchyma, dAVF are shunts supplied by meningeal branches that drain directly into dural veins and/or sinuses. Although most are idiopathic, some dAVFs are evidently acquired in the setting of prior craniotomy, trauma, or dural venous sinus thrombosis. It is thought that AV shunts between meningeal arteries and dural venous sinuses enlarge due to increased pressures, or may form as a result of neoangiogenesis due to outflow obstruction and venous hypertension.<sup>28</sup> Imaging findings vary, but typically present as prominent, tortuous cortical veins in the subarachnoid space, due to retrograde venous flow. Abnormal arterialization in adjacent dural venous sinus may be seen as flow-related enhancement<sup>29–31</sup> (Figure 3).

MRA is variably sensitive to dAVF: one study of 51 dAVFs found MRA to be 50% sensitive,<sup>32</sup> another with 11 dAVFs found MRA was 91% sensitive.<sup>30</sup> Pitfalls of TOF-MRA techniques include overdiagnosis when misinterpreting superiorly flowing venous blood for arterialized flow, or lack of a saturation band leading to enhanced venous flow. Limitations include lack of hemodynamic information and poor visualization of veins.

As venous drainage is the most important factor in symptom severity and risk of complications,<sup>28</sup> full evaluation requires additional imaging (beyond MRA) to fully interrogate venous involvement and hemodynamics. The Borden<sup>33</sup> and Cognard<sup>34</sup> grading systems were devised to stratify lesions based on venous drainage patterns; higher grades demonstrate retrograde cortical venous drainage, are more likely to present with hemorrhage or neurologic compromise, and require more aggressive treatment. As such, any incidental MRA finding suggesting dAVF should be further investigated. This may include contrast-enhanced MRI, MR venogram, or CTA and CT venogram if MR findings are equivocal. Advanced MRA techniques may be appropriate



Figure 3. Dural arteriovenous fistula. (a, b) Axial TOF MRA images performed on a patient with prior history of meningioma involving the superior sagittal sinus. Early flow-related enhancement in the dural venous sinus at the left transverse-sigmoid junction (a, large arrow), with adjacent transosseous venous collaterals (a, arrowhead), compatible with arteriovenous shunting. Prominent cortical veins with flow-related enhancement suggest venous backflow (b, small arrows). (c, d) Follow-up left external carotid artery injection DSA more fully demonstrates the dAVF, including the fistula nidus in which the middle meningeal artery branches empty directly into the transverse/sigmoid sinus (curved arrow), early filling of the left transverse sinus (black arrows), adjacent transosseous collaterals (arrowhead) and prominent cortical veins (small arrows). dAVF, dural arteriovenous fistula; DSA, digital subtraction angiography; MRA, MR angiography; TOF, time-of-flight.

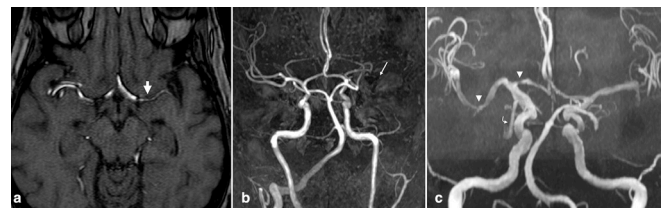


when available, including time resolved or digital subtraction MRA.<sup>35,36</sup> DSA is the gold-standard (providing real-time visualization of the shunt and cortical venous drainage patterns) and should ultimately be performed in any case in which dAVF is considered,<sup>36,37</sup> given that treatment relies on endovascular occlusion.

### Intracranial atherosclerosis

The most common cause of intracranial arterial narrowing is intracranial atherosclerotic disease (ICAD). Luminal stenosis caused by ICAD is most frequently seen in the MCA, followed by the basilar artery (BA), ICA, and intracranial vertebral arteries (VA), typically involving proximal segments and near bifurcations.

Figure 4. Intracranial atherosclerosis. (a) Axial TOF MRA demonstrates segmental high-grade stenosis of the left M1 MCA segment (large arrow), due to ICAD. (b) Minimal flow-related enhancement seen on the axial source image is not well seen on the 3D MIP reconstruction, appearing as an occlusion (small arrow). The contralateral side demonstrates normal MCA caliber. An absent left intracranial VA was also incidentally noted, a benign variant. Of note, subsequent VWI confirmed diagnosis of ICAD (not shown). (c) 3D MIP TOF-MRA reconstruction from a different patient demonstrates multifocal ICAD, e.g. at the proximal A1 and distal M1 segments (arrowheads). A fetal origin of the right PCA was also incidentally noted (curved arrow). MIP, maximum intensity projection; ICAD, intracranial atherosclerotic disease; MCA, middle cerebral artery; MRA, MR angiography; PCA, posterior cerebral artery; VWI, vessel wall MR imaging; TOF, time-of-flight.



ICAD is more prevalent in older patients; on autopsy, severe ICAD is seen in approximately 40% of those in their 60s and 80% of those in their 80s, depending on the specific population.<sup>38</sup> While symptomatic and imaging-detectable ICAD is less prevalent than that, it still represents one of the most common etiologies of stroke.<sup>38,39</sup> Risk factors include hypertension, diabetes, hyperlipidemia, smoking, and age. Treatment strategies primarily involve pharmacologic and lifestyle modifications; surgical and endovascular management are reserved for refractory cases, and performed sparingly.<sup>40</sup>

Imaging characteristics that inform stroke risk include stenosis degree and collateral circulation. While stenosis >70% has been shown to increase risk of recurrent stroke in the affected territory,<sup>41</sup> the presence of robust collaterals mitigates that risk.<sup>42</sup> The main findings indicative of ICAD on MRA are focal, segmental, or multifocal luminal stenoses (Figure 4). Non-contrast TOF-MRA, (although less sensitive for mild disease), has been shown to be 92% sensitive and 91% specific for stenoses >50%.<sup>43</sup> CTA is likely more accurate, and has been reported to have a 97% sensitivity, 99.5% specificity, 93% positive-predictive value, and 99.8% negative-predictive value for ICAD stenosis >50%.<sup>38</sup>

When discovered incidentally, the location and degree of stenosis should be described, as early detection may guide treatment while the disease is still asymptomatic. Assessment of collateral circulation is limited on non-contrast MRA, due to poor visualization of small vessels. Given slightly improved accuracy of CTA (and less susceptibility to flow-related artifacts), follow-up CTA may be considered in equivocal cases. Of note, VWI is likely more sensitive to stenoses than TOF-MRA<sup>44</sup> and CTA,<sup>45</sup> and can also help differentiate atherosclerosis from other causes of luminal narrowing.<sup>46,47</sup> Additionally, VWI can delineate high-risk ICAD features, such as disrupted fibrous cap, intraplaque hemorrhage,

and plaque enhancement,<sup>48,49</sup> which can risk-stratify patients and lead to more aggressive treatment plans.<sup>39</sup>

### Non-atherosclerotic internal carotid artery calcification

The smooth calcifications often seen in the carotid siphons represent a distinct (although often co-existing) pathologic entity from atherosclerosis.<sup>50,51</sup> Non-atherosclerotic calcifications are present in the media and internal elastic lamina, as opposed to the intimal calcifications of focal plaque. Although these calcifications are poorly seen on MRA, they may be inferred by smooth luminal narrowing and/or low-signal wall thickening at the cavernous and paraclinoid segments. Although their significance is not entirely clear, they are likely to be discovered incidentally, and likely confer less stroke risk than true ICAD.<sup>51–54</sup> If there is uncertainty as to the etiology of ICA siphon narrowing on MRA, CTA can confirm the nature of the calcifications and patent lumen.

### Dissection

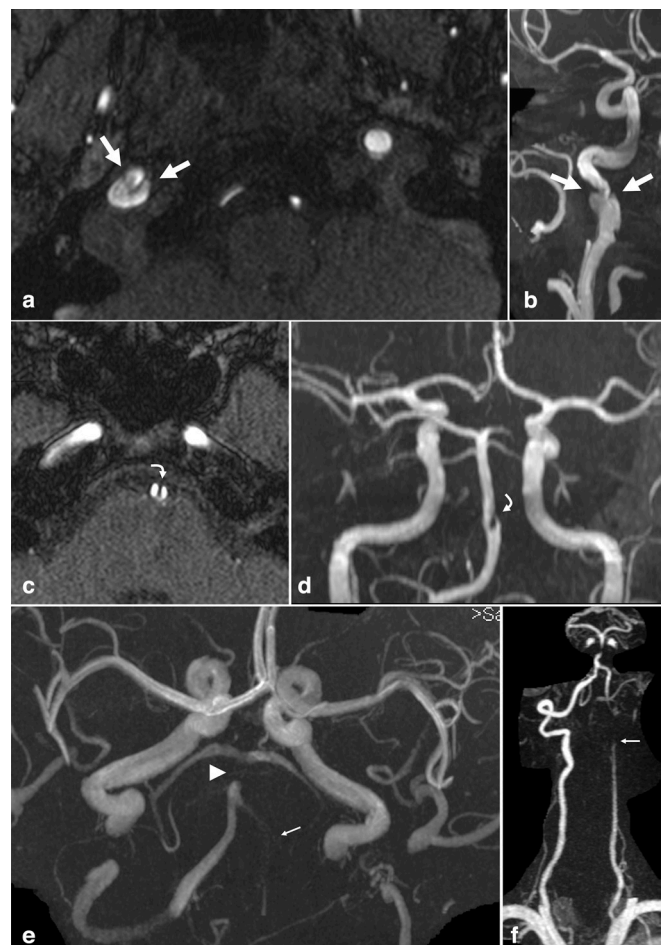
Arterial dissection is characterized by disruption of the endothelium and intima, with blood products extending longitudinally between mural layers.<sup>55</sup> This may lead to a false lumen with displaced intimal flap and/or intramural hematoma, which can result in stenosis of the true lumen, distal thromboembolism, and downstream ischemia. Adventitial-side dissection may lead to intramural hematoma, pseudoaneurysm, luminal stenosis/occlusion, and subarachnoid hemorrhage when intradural.

Dissection may be constrained to the intracranial space, or start extracranially and extend intracranially. Pure intracranial dissections (ICD) are less common (2–3 per 100,000 people per year in those of European ethnic origin) than extracranial dissections.<sup>56</sup> The posterior circulation is more frequently affected, usually involving the V4 segment of the VA.<sup>56,57</sup> Although cervicocerebral trauma is a well-established risk factor for cervical dissections,<sup>58</sup> risk factors for ICD are unknown.<sup>59</sup> Incidence of asymptomatic or incidental ICD is unknown, but approximately 20–50% of all ICDs present with subarachnoid hemorrhage.<sup>56,59</sup> As with cervical dissections, non-traumatic, incidental ICDs may result from underlying connective tissue disorders or unrecognized remote injury.

Historically, MRA has not been considered an appropriate tool for screening of cerebrovascular injuries, with sensitivities inferior to CTA.<sup>58</sup> However, TOF-MRA may demonstrate a linear luminal hypointensity representing a displaced intimal flap, or manifest as a tapering stenosis/occlusion when the false lumen is thrombosed or does not have adequate velocity to produce flow-related enhancement on TOF-MRA (Figure 5). An associated pseudoaneurysm may manifest as fusiform or focal arterial dilatation.

In isolation, TOF-MRA is limited for evaluation of dissection. Stenoses and occlusions may be caused by atherosclerosis, and apparent pseudoaneurysm may represent post-stenotic dilatation. Anatomic variation presents another pitfall; congenitally hypoplastic VAs may be confused for dissection.

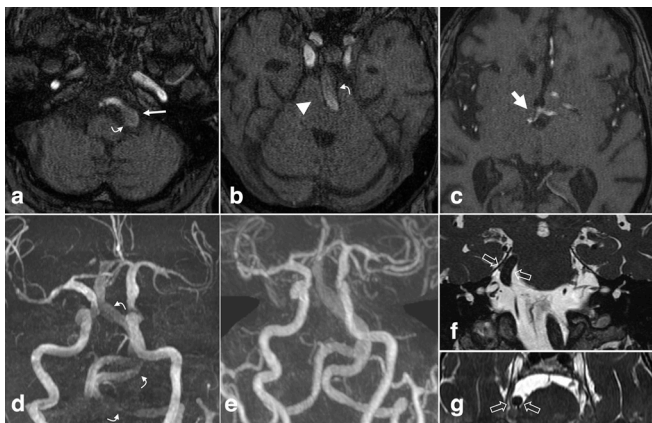
Figure 5. Dissection. (a) Axial TOF-MRA and (b) 3D MIP reconstruction demonstrate an irregular, linear, luminal hypointensity with focal dilatation of the distal cervical ICA at the skull base (large arrows), representing intimal flap and pseudoaneurysm in the setting of dissection. (c) Axial TOF-MRA and (d) 3D MIP reconstruction from a different patient demonstrate an intimal flap of the BA with luminal irregularity (curved arrows). Subsequent VWI confirmed associated intramural hematoma, excluding a variant fenestration (not shown). (e) 3D MIP TOF-MRA in a different patient demonstrates an absent intracranial left VA (small arrow), and occlusion of the mid BA (arrowhead). (f) The contrast-enhanced neck MRA demonstrated tapering and occlusion of the left cervical VA, compatible with dissection (small arrow). BA, basilar artery; ICA, inferior cerebellar artery; MIP, maximum intensity projection; MRA, MR angiography; VA, vertebral artery; VWI, vessel wall MR imaging; TOF, time-of-flight.



Contrast-enhanced neck MRA or CTA are helpful in defining variant anatomy. CTA is better suited for demonstrating a displaced intimal flap given lack of flow-related artifacts. Conventional MRI may demonstrate a loss of flow void, or a crescentic hyperintensity in the false lumen on fat-saturated  $T_1$  weighted or proton-density-weighted sequences. Finally, VWI may be useful in delineating mural abnormalities including intramural hematoma, as well as differentiating from other vasculopathies.<sup>60</sup>



Figure 6. Vertebrobasilar dolichoectasia. (a-c) Non-contrast axial TOF MRA and (d) 3D MIP reconstruction demonstrate diffuse distension, tortuosity, and elongation of the vertebrobasilar arteries. The BA measured up to 9 mm at the base. Note mass effect on the medulla and pons (b, arrowhead). The vertebrobasilar junction is laterally displaced beyond the left lateral margin of the clivus (a, small arrow). The height of the BA bifurcation is above the suprasellar cistern, abutting the hypothalamus (c, large arrow). Slow flow within the ectatic vessel attenuates flow-related enhancement and may mimic thrombus (a, b, d curved arrows). (e) Post-contrast 3D MIP from the concurrent head and neck MRA shows normal luminal patency. Coronal (f) and axial (g) high-resolution T2 weighted images in a different patient with dolichoectasia demonstrate displacement and compression of the cisternal trigeminal nerve due to a tortuous and lateralized BA (open arrows). BA, basilar artery; MIP, maximum intensity projection; MRA, MR angiography; TOF, time-of-flight.



### Dolichoectasia

Dolichoectasia is an uncommon vasculopathy characterized by elongation, tortuosity, and fusiform distension. It is thought to be a degenerative arteriopathy with abnormal connective tissue and vascular remodeling.<sup>61,62</sup> This may predispose to hemodynamic and hemostatic changes, which can result in thrombosis, embolization, or mass effect on adjacent brainstem or cranial nerves.

The exact prevalence is unknown but seems to increase with age and cardiovascular risk factors.<sup>63</sup> The prevalence in symptomatic stroke populations has been reported between 2 and 7%,<sup>64–66</sup> while an MRA-based study of asymptomatic patients in Japan had a prevalence of 1.3%.<sup>67</sup> Most with dolichoectasia are asymptomatic and findings are usually discovered incidentally.

The vertebrobasilar arteries are the most commonly affected, although dolichoectasia of the anterior circulation has also been described.<sup>64</sup> Proposed diagnostic criteria include ectasia (BA diameter >4.5 mm), tortuosity (BA extending lateral to the clivus/dorsum sellae), and length (BA bifurcation height above the suprasellar cistern)<sup>68–70</sup> (Figure 6). Note that on TOF-MRA, slow flow within the ectatic vessel may artifactually attenuate intraluminal signal, leading to false suggestion of stenosis/occlusion.

In nearly all cases, dolichoectasia is an incidental finding requiring no further evaluation. However, if there is concern for compression of adjacent structures, high-resolution 3D T2 weighted images can better evaluate the relationship of vasculature to the cisternal cranial nerves and adjacent brainstem.

### VARIANTS

Appreciation of common vascular variations is important for evaluating the significance of infundibula, collateral circulation, and absent or narrowed luminal signal, and may help avoid unnecessary follow-up imaging, treatment, and patient anxiety. The most prevalent variations are described.

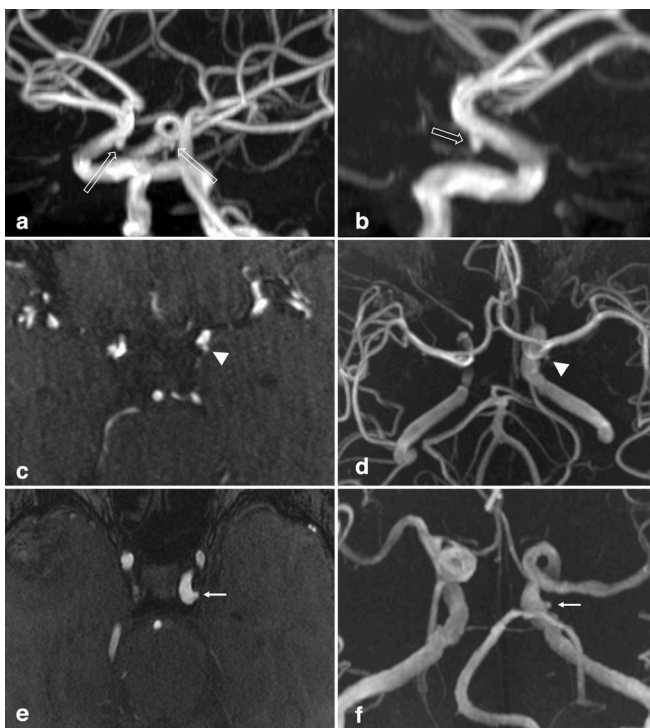
#### Infundibulum

Infundibula are one of the most common incidental findings on MRA, and occur most frequently at the branches of the terminal ICA, at the origins of the posterior communicating (PCoA) and anterior choroidal arteries.<sup>71</sup> An infundibulum is a conical, triangular, or funnel-shaped outpouching at an arterial branch origin (Figure 7); the base faces the ICA (or other parent vessel), while the branch artery emanates from the apex.<sup>71,72</sup> In contrast, a true aneurysm usually bulges asymmetrically from a well-defined neck.<sup>73</sup>

Infundibula are common, found on 7–25% of otherwise normal angiograms.<sup>71,74,75</sup> When present, infundibula are bilateral ~25% of the time.<sup>75</sup> Some have postulated that infundibula may be precursors to aneurysm, while others refute this theory.<sup>76,77</sup> Histologic analysis is mixed; some infundibula show aneurysm-type changes in the arterial wall, while others do not.<sup>78</sup> A handful of reports demonstrate progression to aneurysm, and a few reports describe infundibulum rupture without aneurysm formation.<sup>73</sup> Although unclear, it may be that infundibula are predisposed to further dilation or rupture based on local hemodynamics.<sup>79</sup>

Given a relatively large prevalence and rare reports of progression, infundibula can generally be assumed to represent benign, incidental anatomic variants, especially when small (<3 mm); the majority will undergo no change over time. Unfortunately, while a small, conically shaped outpouching is highly suggestive, an emanating vessel is not always evident, making it difficult to distinguish from pathologic aneurysm. When larger or rounder, it may be difficult to distinguish if the branch vessel emanates apically (infundibulum) or eccentrically (aneurysm). Of note, a well-developed PCoA is seen only in cases of PCoA aneurysm, while infundibula always have small or imperceptible PCoA.<sup>80</sup> A smaller size (<3.45 mm), smaller diameter of emanating PCoA (<1.24 mm), and larger (less acute) angle between the terminal ICA and PCoA are indicative of infundibulum over aneurysm.<sup>81</sup> In equivocal cases, high resolution CTA or DSA may be necessary to identify the branch vessel and make a definitive diagnosis. Regardless, if the infundibulum is large (>3 mm), or if the question of aneurysm vs infundibulum cannot be resolved, serial follow-up with CTA or MRA may be indicated to ensure stability and exclude aneurysm formation or growth.

Figure 7. Infundibulum. (a) Oblique view of a 3D MIP TOF-MRA of the brain demonstrates bilateral conical/triangular outpouchings projecting inferiorly from the terminal ICA (open arrows). Axial source images (not shown) clearly demonstrated small PCoAs emanated from the outpouchings, compatible with PCoA infundibula. (b) Lateral view of the right anterior circulation shows the 2 mm infundibulum and a faint PCoA (open arrow). (c) Axial TOF-MRA and (d) 3D MIP reconstruction demonstrate a small, 1–2 mm anterior choroidal artery infundibulum (arrowheads). (e) Laterally directed 1–2 mm outpouching from the cavernous ICA was favored to represent infundibulum (small arrows), given that a small vessel was seen emanating from the apex, likely the inferolateral trunk (not shown). ICA, inferior cerebellar artery; MIP, maximum intensity projection; MRA, MR angiography; PCoA, posterior communicating artery; TOF, time-of-flight.



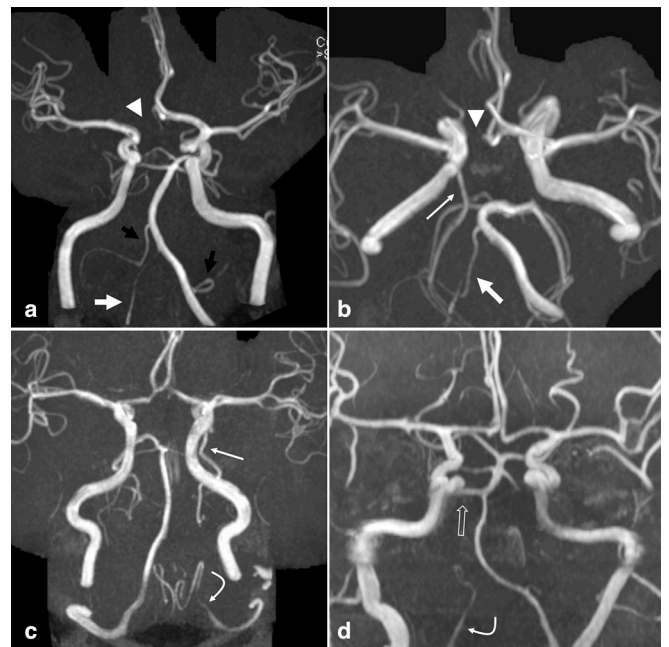
### Hypoplasia and atresia

Any number of the intracranial arteries may be congenitally absent or asymmetrically hypoplastic. It is important to differentiate variant hypoplasia and atresia from acquired occlusion or stenosis, which may require visualization of the entire course of the artery (to assure smooth luminal margins along the entire length, without abrupt caliber change) and evaluation of adjacent bony structures on CT.

### Incomplete Circle of Willis

The Circle of Willis (COW) is a communicating arterial pathway connecting the bilateral anterior and posterior circulation, allowing for collateral supply in the setting of diminished flow from an individual artery. A complete configuration of the COW is present in 42–52%.<sup>82–84</sup> Incomplete COW is an extremely common, normal anatomic variant; a myriad of possible configurations exist. Relative to those with a complete

Figure 8. Variant hypoplasia and atresia. (a) Frontal and (b) transverse views of a 3D MIP TOF-MRA demonstrate common anatomic variations including a dominant left VA and hypoplastic right VA (large white arrows), absent A1 ACA segment on the right (arrowheads), partial fetal PCA on the right (small white arrow), and absent PCoA on the left. Also note a dominant AICA-PICA on the right, and dominant PICA-AICA on the left (a, black arrows). (c) In a separate patient, 3D MIP TOF-MRA demonstrates an absent left V4 VA, with termination as the left PICA (curved arrow); a left fetal PCA is also seen (small white arrow). (d) 3D MIP TOF-MRA in a different patient demonstrates termination of the right VA in PICA (curved arrow), as well as a persistent trigeminal artery on the right (open arrow). ACA, anterior cerebral artery; AICA, anterior inferior cerebellar artery; MIP, maximum intensity projection; MRA, MR angiography; PCA, posterior cerebral artery; PICA, posterior inferior cerebellar artery; TOF, time-of-flight; VA, vertebral artery.



anastomotic circle, an incomplete COW increases risk for ischemia in cases of cervical vessel occlusion or decreased blood flow.

Absence of the communicating arteries is commonly seen. In one study, absence of the bilateral PCoAs was seen in 8–12%, absence of at least one PCoA in 38–48%, and absence of the ACoA in 14–22% of cases.<sup>83</sup> However, it should be noted that in some cases, PCoAs may be too small to produce flow related enhancement on TOF-MRA, and might be identified in the same patients on DSA or CTA.

An absent or hypoplastic A1 segment ACA, with bilateral A2 segments exclusively or predominantly supplied by a single A1 segment is a very common variant, seen in approximately 10% of patients<sup>83</sup> (Figure 8).

Figure 9. Bilateral fetal origin of the PCA. (a) Axial and (b) frontal views of a 3D MIP TOF-MRA reconstruction demonstrate fetal origins of the bilateral PCAs, supplied by prominent PCoAs (large arrows). A small left P1 PCA contribution from the BA is compatible with partial fetal PCA (arrowhead); complete fetal PCA is seen on the right. Note that in the setting of fetal PCAs, the BA is often hypoplastic (small arrow). ACA, anterior cerebral artery; BA, basilar artery; MIP, maximum intensity projection; MRA, MR angiography; PCA, posterior cerebral artery; TOF, time-of-flight.



#### Fetal origin of the PCA

A fetal origin of the posterior cerebral artery (PCA) is the most common variant of the COW, estimated to be present in 20–32%.<sup>85,86</sup> If the embryonic fetal PCoA fails to regress, blood supply to the PCA territory will be dependent upon the ICA. This is variably termed a fetal PCoA, fetal PCA, or fetal origin of the PCA.<sup>82,85,87,88</sup> If the P1 PCA segment from the BA is absent, it can be termed a *complete* fetal PCA; if present but smaller in caliber than the PCoA, it can be termed a *partial* fetal PCA.<sup>82</sup> When fetal PCA is bilateral, the BA is usually diminutive, and terminates in bilateral superior cerebellar arteries (SCAs) (Figure 9).

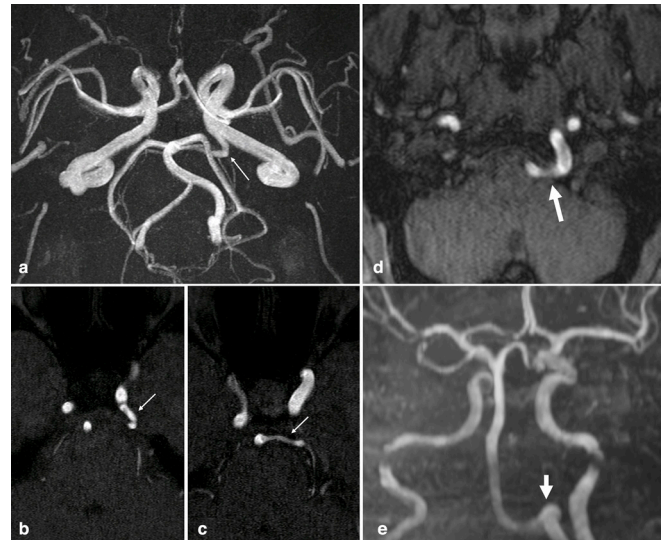
#### Vertebrobasilar asymmetry

True co-dominance of the VAs (in which the bilateral VAs are symmetric in caliber), is rare, and asymmetry common. Hypoplasia (a congenitally diminutive VA) is present on the right in 7–20% and on the left in 6–15%<sup>89,90</sup> (Figure 8). A small V4 VA may minimally contribute to the BA; alternatively, the VA may terminate as posterior inferior cerebellar artery (PICA), which is referred to as VA atresia and seen in approximately 6–18%.<sup>89,91</sup> It is important to not mistake a hypoplastic or atretic VA for a pathologic dissection; in equivocal cases, it may be necessary to evaluate the neck vessels. Neck CTA will better demonstrate osseous structures, including the telling presence of asymmetrically small transverse foramina in cases of hypoplasia. Note that hypoplastic VA has been described as a predisposing factor for posterior circulation infarct.<sup>92</sup>

#### Common trunk variants

In conjunction with VA asymmetry, asymmetry of the cerebellar vessels is common. There may be unilateral atresia of a PICA trunk, with the contralateral PICA or ipsilateral anterior inferior cerebellar artery (AICA), termed an AICA–PICA, supplying the normal territory of the PICA. Likewise, when the AICA trunk is atretic, the ipsilateral PICA may supply the AICA territory, termed PICA–AICA (Figure 8).

Figure 10. Persistent vertebrobasilar anastomoses. (a) 3D MIP reconstruction and (b, c) axial TOF-MRA source images demonstrate a left-sided persistent trigeminal artery, emanating from the left cavernous ICA and anastomosing with the BA (small arrows). (d) Axial TOF-MRA and (e) 3D MIP reconstruction in another patient demonstrate a left-sided persistent hypoglossal artery, emanating from the left cervical ICA, traversing the hypoglossal canal (large arrows), and continuing as the basilar artery. The bilateral VAs were markedly hypoplastic. BA, basilar artery; ICA, internal carotid artery; MIP, maximum intensity projection; MRA, MR angiography; TOF, time-of-flight; VA, vertebral artery.



The PCA and SCA may originate from a common trunk at the terminus of the BA in 2–22% of patients.<sup>87,88</sup> Although of no clinical significance, the presence of a common trunk may appear as a focal dilatation and should not be mistaken for aneurysm.

#### Internal carotid hypoplasia and agenesis

Congenitally hypoplastic or absent ICA is rare, and may be associated with other developmental anomalies. Prevalence of complete ICA atresia is 0.1%.<sup>87,88</sup> When a hypoplastic or absent ICA is suspected on MRA, a CT demonstrating small or absent carotid canal is confirmatory of the congenital variant. CTA can also more definitively demonstrate congenital hypoplasia/absence, which should not be mistaken for acquired or pathologic narrowing.

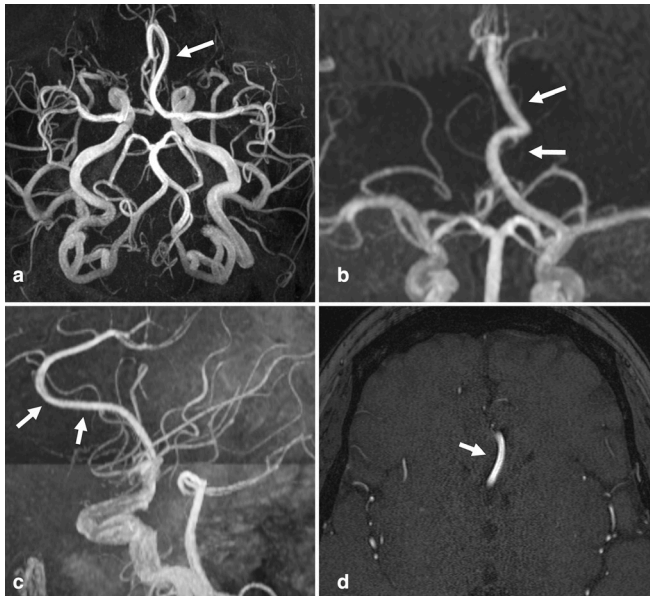
#### Carotid-vertebrobasilar anastomoses

Persistent fetal carotid-vertebrobasilar anastomoses are remnants of the embryonic blood supply in which the ICA supplies the primitive vertebrobasilar system.<sup>93</sup> The trigeminal, otic, hypoglossal, and proatlantal arteries, (named for neighboring structures), normally recede as the vertebrobasilar system develops, but rarely persist into adult life.

Persistent trigeminal artery (PTA) is the most common variation, seen in 0.1–1.0%.<sup>87,88,94</sup> PTA usually originates at the posterior bend of the intracavernous ICA, connecting posteriorly to the BA between the SCA and AICA<sup>95</sup> (Figure 10). When joining



Figure 11. Azygous anterior cerebral artery. (a) Axial oblique, (b) frontal, and (c) lateral views of a 3D MIP TOF-MRA, as well as (d) an axial TOF-MRA source image demonstrate an incidental single prominent midline ACA supplying the bilateral A3 branches (arrows). In this case, the large azygous artery is a continuation of the left A1 segment. A small right A1 segment supplied only a small orbitofrontal branch. MIP, maximum intensity projection; MRA, MR angiography; TOF, time-of-flight.



directly to the SCA or PICA, it is termed a PTA variant.<sup>87,95</sup> Approximately, 50% of the time, the PTA penetrates the sella turcica near the clivus to join the BA; otherwise, it travels lateral to the sella within the cavernous sinus. Describing its course is important in cases of transphenoidal surgery, in order to avoid operative PTA injury and devastating hemorrhage.

A persistent otic artery is an extremely rare observation, and when reported, is often questioned. It provides only minor supply to the developing vertebrobasilar system and is the first of the anastomoses to regress embryologically.<sup>93</sup> If present, it arises from the petrous ICA and passes through the internal auditory canal to the BA.

The persistent hypoglossal artery is the second most common fetal carotid-vertebrobasilar anastomosis (prevalence~0.1–0.25%),<sup>88</sup> originating from the cervical ICA, traversing the hypoglossal canal medial to the hypoglossal nerve, and anastomosing with the BA just distal to its origin. There may be associated enlargement of the hypoglossal canal and hypoplasia of the ipsilateral or bilateral VAs<sup>93,94</sup> (Figure 10).

The persistent proatlantal artery is the most caudal fetal vertebrobasilar anastomosis, and may be seen on the inferior limits of a brain MRA exam. When present, it may originate from the cervical ICA or external carotid artery, anastomosing with the VA in the suboccipital region near the foramen magnum.<sup>87,93,94</sup> The VA proximal to the anastomoses is usually hypoplastic.

Figure 12. Basilar artery fenestration. (a) Axial TOF MRA (b) frontal 3D MIP reconstruction demonstrate a linear luminal flow void at the base of the BA (arrow). Although appearance on axial images is similar to that of an intimal flap in the setting of dissection, and dilated appearance on 3D MIP (arrowhead) is similar to a dissecting aneurysm, location and short segment involvement are suggestive of a fenestration, a benign developmental variant. If findings on TOF MRA are equivocal, CTA or DSA can confirm. CTA, CT angiography; DSA, digital subtraction angiography; MIP, maximum intensity projection; MRA, MR angiography; TOF, time-of-flight.



#### Azygous anterior cerebral artery

Persistence of the embryonic median artery of the corpus callosum leads to what is known as an azygous ACA: a single, prominent midline A2 segment supplying the bilateral ACA territories. The prevalence is 0.2–4%.<sup>87</sup> Azygous ACA may be associated with other developmental anomalies, as well as increased incidence of aneurysm at its interhemispheric bifurcation<sup>85</sup> (Figure 11).

#### Fenestrations and Duplications

A fenestrated artery is characterized by division of the lumen into two distinct channels (with proximal and distal convergence), while a duplicated artery is one that is represented by two distinct origins with no distal convergence. Fenestration can occur anywhere but is most common at the ACoA (5–21%), BA (0.6–5%), and VAs (0.3–2.0%).<sup>87</sup> BA fenestrations are usually seen at the proximal trunk and are associated with aneurysm 7% of the time.<sup>96</sup> Accurate diagnosis is significant; on poor quality or low-resolution studies the focal luminal divergence of a fenestration may be mistaken for dissection or aneurysmal dilatation (Figure 12).

Duplication can also occur almost anywhere, but the SCA (~22%)<sup>97</sup> and ACoA (18%) are most common.<sup>98</sup> True MCA duplication is rare (0.2–3%)<sup>85</sup>; apparent MCA duplication is referred to as an “accessory” MCA when it originates from the ACA rather than the ICA, and other apparent MCA duplications may represent early branching, with a short M1 segment.

#### CONCLUSION

Incidental vascular findings discovered on MRA may represent asymptomatic pathology, benign lesions, or variant anatomy. Understanding the prevalence, clinical significance, and important imaging features of common vascular pathology helps the diagnostician to guide surveillance and treatment.

Appreciating the characteristics and prevalence of common anatomic variants allows the patient to avoid unnecessary treatment and follow-up imaging.

## AUTHOR DISCLOSURES

All authors have no conflicts of interest to disclose and there were no financial incentives that would alter the contents of this manuscript.

## REFERENCES

- Vlak MH, Algra A, Brandenburg R, Rinkel GJ. Prevalence of unruptured intracranial aneurysms, with emphasis on sex, age, comorbidity, country, and time period: a systematic review and meta-analysis. *Lancet Neurol* 2011; **10**: 626–36. [https://doi.org/10.1016/S1474-4422\(11\)70109-0](https://doi.org/10.1016/S1474-4422(11)70109-0)
- Backes D, Rinkel GJE, Laban KG, Algra A, Vergouwen MDI. Patient- and aneurysm-specific risk factors for intracranial aneurysm growth. *Stroke* 2016; **47**: 951–57. <https://doi.org/10.1161/STROKEAHA.115.012162>
- Thompson BG, Brown RD Jr, Amin-Hanjani S, Broderick JP, Cockroft KM, Connolly ES Jr, et al. Guidelines for the management of patients with unruptured intracranial aneurysms. *Stroke* 2015; **46**: 2368–2400. <https://doi.org/10.1161/STR.0000000000000070>
- Go AS, Mozaffarian D, Roger VL, Benjamin EJ, Berry JD, Blaha MJ, et al. Executive summary: heart disease and stroke statistics—2014 update. *Circulation* 2014; **129**: 399–410. <https://doi.org/10.1161/01.cir.0000442015.53336.12>
- Gawlitza M, Soize S, Barbe C, le Clainche A, White P, Spelle L, et al. Aneurysm characteristics, study population, and endovascular techniques for the treatment of intracranial aneurysms in a large, prospective, multicenter cohort: results of the analysis of recanalization after endovascular treatment of intracranial aneurysm study. *AJNR Am J Neuroradiol* 2019; **40**: 517–23. <https://doi.org/10.3174/ajnr.A5991>
- Inagawa T. Risk factors for the formation and rupture of intracranial saccular aneurysms in shimane, japan. *World Neurosurg* 2010; **73**: 155–64. <https://doi.org/10.1016/j.surneu.2009.03.007>
- Juvela S, Poussa K, Porras M. Factors affecting formation and growth of intracranial aneurysms: a long-term follow-up study. *Stroke* 2001; **32**: 485–91. <https://doi.org/10.1161/01.str.32.2.485>
- Kissela BM, Sauerbeck L, Woo D, Khoury J, Carrozzella J, Pancioli A, et al. Subarachnoid hemorrhage: a preventable disease with a heritable component. *Stroke* 2002; **33**: 1321–26. <https://doi.org/10.1161/01.str.0000014773.57733.3e>
- Salmela MB, Mortazavi S, Jagadeesan BD, Broderick DF, Burns J, Deshmukh TK, et al. ACR appropriateness criteria © cerebrovascular disease. *Journal of the American College of Radiology* 2017; **14**: S34–61. <https://doi.org/10.1016/j.jacr.2017.01.051>
- Sailer AMH, Wagemans BAJM, Nelemans PJ, de Graaf R, van Zwam WH. Diagnosing intracranial aneurysms with MR angiography: systematic review and meta-analysis. *Stroke* 2014; **45**: 119–26. <https://doi.org/10.1161/STROKEAHA.113.003133>
- Li M-H, Li Y-D, Gu B-X, Cheng Y-S, Wang W, Tan H-Q, et al. Accurate diagnosis of small cerebral aneurysms ≤5 mm in diameter with 3.0-T MR angiography. *Radiology* 2014; **271**: 553–60. <https://doi.org/10.1148/radiol.14122770>
- Abulhasan YB, Alabdulraheem N, Simoneau G, Angle MR, Teitelbaum J. Mortality after spontaneous subarachnoid hemorrhage: causality and validation of a prediction model. *World Neurosurg* 2018; **112**: e799–811: S1878-8750(18)30203-1. <https://doi.org/10.1016/j.wneu.2018.01.160>
- van Gijn J, Kerr RS, Rinkel GJE. Subarachnoid haemorrhage. *Lancet* 2007; **369**: 306–18. [https://doi.org/10.1016/S0140-6736\(07\)60153-6](https://doi.org/10.1016/S0140-6736(07)60153-6)
- Brinjikji W, Zhu Y-Q, Lanzino G, Cloft HJ, Murad MH, Wang Z, et al. Risk factors for growth of intracranial aneurysms: A systematic review and meta-analysis. *AJNR Am J Neuroradiol* 2016; **37**: 615–20. <https://doi.org/10.3174/ajnr.A4575>
- Mocco J, Brown RD Jr, Torner JC, Capuano AW, Fargen KM, Raghavan ML, et al. Aneurysm morphology and prediction of rupture: an international study of unruptured intracranial aneurysms analysis. *Neurosurgery* 2018; **82**: 491–96. <https://doi.org/10.1093/neuros/nyx226>
- Lehman VT, Brinjikji W, Mossa-Basha M, Lanzino G, Rabinstein AA, Kallmes DE, et al. Conventional and high-resolution vessel wall MRI of intracranial aneurysms: current concepts and new horizons. *J Neurosurg* 2018; **128**: 2016.12.JNS162262: 969–81. <https://doi.org/10.3171/2016.12.JNS162262>
- Zhu C, Mossa-Basha M. Wall enhancement as an emerging marker of intracranial aneurysm stability: roadmap toward a potential target for clinical trials. *Eur J Neurol* 2021; **28**: 3550–51. <https://doi.org/10.1111/ene.15094>
- Al-Shahi R, Warlow C. A systematic review of the frequency and prognosis of arteriovenous malformations of the brain in adults. *Brain* 2001; **124**: 1900–1926. <https://doi.org/10.1093/brain/124.10.1900>
- Lawton MT, Rutledge WC, Kim H, Stapf C, Whitehead KJ, Li DY, et al. Brain arteriovenous malformations. *Nat Rev Dis Primers* 2015; **1**: 15008. <https://doi.org/10.1038/nrdp.2015.8>
- Can A, Gross BA, Du R. The natural history of cerebral arteriovenous malformations. *Handb Clin Neurol* 2017; **143**: B978-0-444-63640-9.00002-3: 15–24. <https://doi.org/10.1016/B978-0-444-63640-9.00002-3>
- Stapf C, Mast H, Sciacca RR, Choi JH, Khaw AV, Connolly ES, et al. Predictors of hemorrhage in patients with untreated brain arteriovenous malformation. *Neurology* 2006; **66**: 1350–55. <https://doi.org/10.1212/01.wnl.0000210524.68507.87>
- Yamada S, Takagi Y, Nozaki K, Kikuta K, Hashimoto N. Risk factors for subsequent hemorrhage in patients with cerebral arteriovenous malformations. *J Neurosurg* 2007; **107**: 965–72. <https://doi.org/10.3171/JNS-07/11/0965>
- Gross BA, Frerichs KU, Du R. Sensitivity of CT angiography, T2-weighted MRI, and magnetic resonance angiography in detecting cerebral arteriovenous malformations and associated aneurysms. *J Clin Neurosci* 2012; **19**: 1093–95. <https://doi.org/10.1016/j.jocn.2011.11.021>
- Fukuda K, Majumdar M, Masoud H, Nguyen T, Honarmand A, Shaibani A, et al. Multicenter assessment of morbidity associated with cerebral arteriovenous malformation hemorrhages. *J Neurointerv Surg* 2017; **9**: 664–68. <https://doi.org/10.1136/neurintsurg-2016-012485>
- Karlsson B, Jokura H, Yang H-C, Yamamoto M, Martinez R, Kawagishi J, et al. Clinical outcome following cerebral AVM hemorrhage. *Acta Neurochir (Wien)* 2020;

- 162: 1759–66. <https://doi.org/10.1007/s00701-020-04380-z>
26. Spetzler RF, Martin NA. A proposed grading system for arteriovenous malformations. *J Neurosurg* 1986; **65**: 476–83. <https://doi.org/10.3171/jns.1986.65.4.0476>
  27. Rutledge C, Cooke DL, Hetts SW, Abula AA. Brain arteriovenous malformations. *Handb Clin Neurol* 2021; **176**: B978-0-444-64034-5.00020-1: 171–78. <https://doi.org/10.1016/B978-0-444-64034-5.00020-1>
  28. Gandhi D, Chen J, Pearl M, Huang J, Gemmete JJ, Kathuria S. Intracranial dural arteriovenous fistulas: classification, imaging findings, and treatment. *AJNR Am J Neuroradiol* 2012; **33**: 1007–13. <https://doi.org/10.3174/ajnr.A2798>
  29. Chen C-J, Ding D, Derdeyn CP, Lanzino G, Friedlander RM, Southerland AM, et al. Brain arteriovenous malformations: A review of natural history, pathobiology, and interventions. *Neurology* 2020; **95**: 917–27. <https://doi.org/10.1212/WNL.000000000010968>
  30. Kwon BJ, Han MH, Kang H-S, Chang K-H. MR imaging findings of intracranial dural arteriovenous fistulas: relations with venous drainage patterns. *AJNR Am J Neuroradiol* 2005; **26**: 2500–2507.
  31. Noguchi K, Melhem ER, Kanazawa T, Kubo M, Kuwayama N, Seto H. Intracranial dural arteriovenous fistulas: evaluation with combined 3D time-of-flight MR angiography and MR digital subtraction angiography. *AJR Am J Roentgenol* 2004; **182**: 183–90. <https://doi.org/10.2214/ajr.182.1.1820183>
  32. Cohen SD, Goins JL, Butler SG, Morris PP, Browne JD. Dural arteriovenous fistula: diagnosis, treatment, and outcomes. *Laryngoscope* 2009; **119**: 293–97. <https://doi.org/10.1002/lary.20084>
  33. Borden JA, Wu JK, Shucart WA. A proposed classification for spinal and cranial dural arteriovenous fistulous malformations and implications for treatment. *J Neurosurg* 1995; **82**: 166–79. <https://doi.org/10.3171/jns.1995.82.2.0166>
  34. Cognard C, Gobin YP, Pierot L, Bailly AL, Houdart E, Casasco A, et al. Cerebral dural arteriovenous fistulas: clinical and angiographic correlation with a revised classification of venous drainage. *Radiology* 1995; **194**: 671–80. <https://doi.org/10.1148/radiology.194.3.7862961>
  35. Nishimura S, Hirai T, Sasao A, Kitajima M, Morioka M, Kai Y, et al. Evaluation of dural arteriovenous fistulas with 4D contrast-enhanced MR angiography at 3T. *AJNR Am J Neuroradiol* 2010; **31**: 80–85. <https://doi.org/10.3174/ajnr.A1898>
  36. Noguchi K, Melhem ER, Kanazawa T, Kubo M, Kuwayama N, Seto H. Intracranial dural arteriovenous fistulas: evaluation with combined 3D time-of-flight MR angiography and MR digital subtraction angiography. *AJR Am J Roentgenol* 2004; **182**: 183–90. <https://doi.org/10.2214/ajr.182.1.1820183>
  37. Brown RD, Wiebers DO, Nichols DA. Intracranial dural arteriovenous fistulae: angiographic predictors of intracranial hemorrhage and clinical outcome in nonsurgical patients. *J Neurosurg* 1994; **81**: 531–38. <https://doi.org/10.3171/jns.1994.81.4.0531>
  38. Banerjee C, Chimowitz MI. Stroke caused by atherosclerosis of the major intracranial arteries. *Circ Res* 2017; **120**: 502–13. <https://doi.org/10.1161/CIRCRESAHA.116.308441>
  39. Qureshi AI, Caplan LR. Intracranial atherosclerosis. *Lancet* 2014; **383**: S0140-6736(13)61088-0: 984–98. [https://doi.org/10.1016/S0140-6736\(13\)61088-0](https://doi.org/10.1016/S0140-6736(13)61088-0)
  40. Holmstedt CA, Turan TN, Chimowitz MI. Atherosclerotic intracranial arterial stenosis: risk factors, diagnosis, and treatment. *Lancet Neurol* 2013; **12**: S1474-4422(13)70195-9: 1106–14. [https://doi.org/10.1016/S1474-4422\(13\)70195-9](https://doi.org/10.1016/S1474-4422(13)70195-9)
  41. Kasner SE, Chimowitz MI, Lynn MJ, Howlett-Smith H, Stern BJ, Hertzberg VS, et al. Predictors of ischemic stroke in the territory of a symptomatic intracranial arterial stenosis. *Circulation* 2006; **113**: 555–63. <https://doi.org/10.1161/CIRCULATIONAHA.105.578229>
  42. Liebeskind DS, Cotsonis GA, Saver JL, Lynn MJ, Turan TN, Cloft HJ, et al. Collaterals dramatically alter stroke risk in intracranial atherosclerosis. *Ann Neurol* 2011; **69**: 963–74. <https://doi.org/10.1002/ana.22354>
  43. Hirai T, Korogi Y, Ono K, Nagano M, Maruoka K, Uemura S, et al. Prospective evaluation of suspected stenooclusive disease of the intracranial artery: combined MR angiography and CT angiography compared with digital subtraction angiography. *AJNR Am J Neuroradiol* 2002; **23**: 93–101.
  44. Tian X, Tian B, Shi Z, Wu X, Peng W, Zhang X, et al. Assessment of intracranial atherosclerotic plaques using 3D black-blood MRI: comparison with 3D time-of-flight MRA and DSA. *J Magn Reson Imaging* 2021; **53**: 469–78. <https://doi.org/10.1002/jmri.27341>
  45. Sarikaya B, Colip C, Hwang WD, Hippe DS, Zhu C, Sun J, et al. Comparison of time-of-flight MR angiography and intracranial vessel wall MRI for luminal measurements relative to CT angiography. *Br J Radiol* 2021; **94**(1118): 20200743. <https://doi.org/10.1259/bjr.20200743>
  46. Arenillas JF. Intracranial atherosclerosis: current concepts. *Stroke* 2011; **42**: S20-3. <https://doi.org/10.1161/STROKEAHA.110.597278>
  47. Mossa-Basha M, Shibata DK, Hallam DK, de Havenon A, Hippe DS, Becker KJ, et al. Added value of vessel wall magnetic resonance imaging for differentiation of nonocclusive intracranial vasculopathies. *Stroke* 2017; **48**: 3026–33. <https://doi.org/10.1161/STROKEAHA.117.018227>
  48. Brinjikji W, Mossa-Basha M, Huston J, Rabinstein AA, Lanzino G, Lehman VT. Intracranial vessel wall imaging for evaluation of steno-occlusive diseases and intracranial aneurysms. *J Neuroradiol* 2017; **44**: S0150-9861(16)30173-0: 123–34. <https://doi.org/10.1016/j.neurad.2016.10.003>
  49. Mossa-Basha M, Alexander M, Gaddikeri S, Yuan C, Gandhi D. Vessel wall imaging for intracranial vascular disease evaluation. *J Neurointerv Surg* 2016; **8**: 1154–59. <https://doi.org/10.1136/neurintsurg-2015-012127>
  50. Kockelkoren R, Vos A, Van Hecke W, Vink A, Bley RLAW, Verdoorn D, et al. Computed tomographic distinction of intimal and medial calcification in the intracranial internal carotid artery. *PLoS One* 2017; **12**(1): e0168360. <https://doi.org/10.1371/journal.pone.0168360>
  51. Vos A, Van Hecke W, Spliet WGM, Goldschmeding R, Isgum I, Kockelkoren R, et al. Predominance of nonatherosclerotic internal elastic lamina calcification in the intracranial internal carotid artery. *Stroke* 2016; **47**: 221–23. <https://doi.org/10.1161/STROKEAHA.115.011196>
  52. Erbay S, Han R, Baccei S, Krakov W, Zou KH, Bhadelia R, et al. Intracranial carotid artery calcification on head CT and its association with ischemic changes on brain MRI in patients presenting with stroke-like symptoms: retrospective analysis. *Neuroradiology* 2007; **49**: 27–33. <https://doi.org/10.1007/s00234-006-0159-z>
  53. de Weert TT, Cakir H, Rozie S, Cretier S, Meijering E, Dippel DWJ, et al. Intracranial internal carotid artery calcifications: association with vascular risk factors and ischemic cerebrovascular disease. *AJNR Am J Neuroradiol* 2009; **30**: 177–84. <https://doi.org/10.3174/ajnr.A1301>
  54. Quiney B, Ying SM, Hippe DS, Balu N, Urdaneta-Moncada AR, Mossa-Basha M. The association of intracranial vascular calcification and stenosis with acute ischemic cerebrovascular events. *J Comput Assist Tomogr* 2017; **41**: 849–53. <https://doi.org/10.1097/RCT.0000000000000629>



55. Krings T, Choi I-S. The many faces of intracranial arterial dissections. *Interv Neuroradiol* 2010; **16**: 151–60. <https://doi.org/10.1177/159101991001600206>
56. Dabette S, Compter A, Labeyrie M-A, Uyttenboogaart M, Metso TM, Majersik JJ, et al. Epidemiology, pathophysiology, diagnosis, and management of intracranial artery dissection. *Lancet Neurol* 2015; **14**: S1474-4422(15)00009-5: 640–54. [https://doi.org/10.1016/S1474-4422\(15\)00009-5](https://doi.org/10.1016/S1474-4422(15)00009-5)
57. Metso TM, Metso AJ, Helenius J, Haapaniemi E, Salonen O, Porras M, et al. Prognosis and safety of anticoagulation in intracranial artery dissections in adults. *Stroke* 2007; **38**: 1837–42. <https://doi.org/10.1161/STROKEAHA.106.479501>
58. Rutman AM, Vranic JE, Mossa-Basha M. Imaging and management of blunt cerebrovascular injury. *Radiographics* 2018; **38**: 542–63. <https://doi.org/10.1148/rg.2018170140>
59. Pelkonen O, Tikkakoski T, Pyhtinen J, Sotaniemi K. Cerebral CT and MRI findings in cervicocephalic artery dissection. *Acta Radiol* 2004; **45**: 259–65. <https://doi.org/10.1080/02841850410004184>
60. Vranic JE, Huynh TJ, Fata P, Barber J, Bonow RH, Levitt MR, et al. The ability of magnetic resonance black blood vessel wall imaging to evaluate blunt cerebrovascular injury following acute trauma. *J Neuroradiol* 2020; **47**: S0150-9861(18)30330-4: 210–15. <https://doi.org/10.1016/j.neurad.2019.01.091>
61. Lou M, Caplan LR. Vertebrobasilar dilatative arteriopathy (dolichoectasia). *Ann N Y Acad Sci* 2010; **1184**: 121–33. <https://doi.org/10.1111/j.1749-6632.2009.05114.x>
62. Samim M, Goldstein A, Schindler J, Johnson MH. Multimodality imaging of vertebrobasilar dolichoectasia: clinical presentations and imaging spectrum. *Radiographics* 2016; **36**: 1129–46. <https://doi.org/10.1148/rg.2016150032>
63. Gutierrez J, Sacco RL, Wright CB. Dolichoectasia—an evolving arterial disease. *Nat Rev Neurol* 2011; **7**: 41–50. <https://doi.org/10.1038/nrneurol.2010.181>
64. Vasović L, Trandafilović M, Jovanović I, Ugrešević S, Vlačković S. Vertebral and/or basilar dolichoectasia in human adult cadavers. *Acta Neurochir (Wien)* 2012; **154**: 1477–88. <https://doi.org/10.1007/s00701-012-1400-7>
65. Ince B, Petty GW, Brown RD, Chu CP, Sicks JD, Whisnand JP. Dolichoectasia of the intracranial arteries in patients with first ischemic stroke: a population-based study. *Neurology* 1998; **50**: 1694–98. <https://doi.org/10.1212/wnl.50.6.1694>
66. Kumral E, Kisabay A, Ataç C, Kaya C, Calli C. The mechanism of ischemic stroke in patients with dolichoectatic basilar artery. *Eur J Neurol* 2005; **12**: 437–44. <https://doi.org/10.1111/j.1468-1331.2005.00993.x>
67. Ikeda K, Nakamura Y, Hirayama T, Sekine T, Nagata R, Kano O, et al. Cardiovascular risk and neuroradiological profiles in asymptomatic vertebrobasilar dolichoectasia. *Cerebrovasc Dis* 2010; **30**: 23–28. <https://doi.org/10.1159/000313440>
68. Smoker WR, Corbett JJ, Gentry LR, Keyes WD, Price MJ, McKusker S. High-resolution computed tomography of the basilar artery: 2. vertebrobasilar dolichoectasia: clinical-pathologic correlation and review. *AJNR Am J Neuroradiol* 1986; **7**: 61–72.
69. Förster A, Ssozi J, Al-Zghoul M, Brockmann MA, Kerl HU, Groden C. A comparison of CT/CT angiography and MRI/MR angiography for imaging of vertebrobasilar dolichoectasia. *Clin Neuroradiol* 2014; **24**: 347–53. <https://doi.org/10.1007/s00062-013-0261-7>
70. Giang DW, Perlin SJ, Monajati A, Kido DJ, Hollander J. Vertebrobasilar dolichoectasia: assessment using MR. *Neuroradiology* 1988; **30**: 518–23. <https://doi.org/10.1007/BF00339693>
71. SALTZMAN GF. Patent primitive trigeminal artery studied by cerebral angiography. *Acta Radiol* 1959; **51**: 329–36. <https://doi.org/10.3109/00016925909171103>
72. Pool JL, Potts DG. Aneurysms and arteriovenous anomalies of the brain: Diagnosis and treatment. New York: Harper and Row; 1965.
73. Marshman LAG, Ward PJ, Walter PH, Dossetor RS. The progression of an infundibulum to aneurysm formation and rupture: case report and literature review. *Neurosurgery* 1998; **43**: 1445–48. <https://doi.org/10.1227/00006123-199812000-00107>
74. Ebina K, Ohkuma H, Iwabuchi T. An angiographic study of incidence and morphology of infundibular dilation of the posterior communicating artery. *Neuroradiology* 1986; **28**: 23–29. <https://doi.org/10.1007/BF00341761>
75. Wollschlaeger G, Wollschlaeger PB, Lucas FV, Lopez VF. Experience and result with postmortem cerebral angiography performed as routine procedure of the autopsy. *Am J Roentgenol Radium Ther Nucl Med* 1967; **101**: 68–87. <https://doi.org/10.2214/ajr.101.1.68>
76. Edelsohn L, Caplan L, Rosenbaum AE. Familial aneurysms and infundibular widening. *Neurology* 1972; **22**: 1056–60. <https://doi.org/10.1212/wnl.22.10.1056>
77. HASSLER O, SALTZMAN GF. Histologic changes in infundibular widening of the posterior communicating artery. A preliminary report. *Acta Pathol Microbiol Scand* 1959; **46**: 305–12. <https://doi.org/10.1111/j.1699-0463.1959.tb01100.x>
78. Epstein F, Ransohoff J, Budzilovich GN. The clinical significance of junctional dilatation of the posterior communicating artery. *J Neurosurg* 1970; **33**: 529–31. <https://doi.org/10.3171/jns.1970.33.5.0529>
79. Baek H, Jayaraman MV, Karniadakis GE. Wall shear stress and pressure distribution on aneurysms and infundibulae in the posterior communicating artery bifurcation. *Ann Biomed Eng* 2009; **37**: 2469–87. <https://doi.org/10.1007/s10439-009-9794-y>
80. Endo S, Furuichi S, Takaba M, Hirashima Y, Nishijima M, Takaku A. Clinical study of enlarged infundibular dilation of the origin of the posterior communicating artery. *J Neurosurg* 1995; **83**: 421–25. <https://doi.org/10.3171/jns.1995.83.3.0421>
81. Yuan J, Li Z, Jiang X, Lai N, Wang X, Zhao X, et al. Hemodynamic and morphological differences between unruptured carotid-posterior communicating artery bifurcation aneurysms and infundibular dilations of the posterior communicating artery. *Front Neurol* 2020; **11**: 741. <https://doi.org/10.3389/fneur.2020.00741>
82. van Raamt AF, Mali WPTM, van Laar PJ, van der Graaf Y. The fetal variant of the circle of willis and its influence on the cerebral collateral circulation. *Cerebrovasc Dis* 2006; **22**: 217–24. <https://doi.org/10.1159/000094007>
83. Krabbe-Hartkamp MJ, van der Grond J, de Leeuw FE, de Groot JC, Algra A, Hillen B, et al. Circle of willis: morphologic variation on three-dimensional time-of-flight MR angiograms. *Radiology* 1998; **207**: 103–11. <https://doi.org/10.1148/radiology.207.1.9530305>
84. ALPERS BJ, BERRY RG, PADDISON RM. Anatomical studies of the circle of willis in normal brain. *AMA Arch Neurol Psychiatry* 1959; **81**: 409–18. <https://doi.org/10.1001/archneurpsyc.1959.02340160007002>
85. Zampakis P, Panagiotopoulos V, Petsas T, Kalogeropoulou C. Common and uncommon intracranial arterial anatomic variations in multi-detector computed tomography angiography (MDCTA). what radiologists should be aware of. *Insights Imaging* 2015; **6**: 33–42. <https://doi.org/10.1007/s13244-014-0381-x>
86. Bisaria KK. Anomalies of the posterior communicating artery and their potential clinical significance. *J Neurosurg* 1984; **60**: 572–76. <https://doi.org/10.3171/jns.1984.60.3.0572>

87. Dimmick SJ, Faulder KC. Normal variants of the cerebral circulation at multidetector CT angiography. *Radiographics* 2009; **29**: 1027–43. <https://doi.org/10.1148/rg.294085730>
88. Okahara M, Kiyosue H, Mori H, Tanoue S, Sainou M, Nagatomi H. Anatomic variations of the cerebral arteries and their embryology: a pictorial review. *Eur Radiol* 2002; **12**: 2548–61. <https://doi.org/10.1007/s00330-001-1286-x>
89. Omotoso BR, Harrichandparsad R, Satyapal KS, Moodley IG, Lazarus L. Radiological anatomy of the intracranial vertebral artery in a select south african cohort of patients. *Sci Rep* 2021; **11**(1): 12138. <https://doi.org/10.1038/s41598-021-91744-9>
90. Songur A, Gonul Y, Ozen OA, Kucuker H, Uzun I, Bas O, et al. Variations in the intracranial vertebrobasilar system. *Surg Radiol Anat* 2008; **30**: 257–64. <https://doi.org/10.1007/s00276-008-0309-6>
91. Liu I-W, Ho B-L, Chen C-F, Han K, Lin C-J, Sheng W-Y, et al. Vertebral artery terminating in posterior inferior cerebellar artery: A normal variation with clinical significance. *PLoS One* 2017; **12**(4): e0175264. <https://doi.org/10.1371/journal.pone.0175264>
92. Perren F, Poglia D, Landis T, Sztajzel R. Vertebral artery hypoplasia: A predisposing factor for posterior circulation stroke? *Neurology* 2007; **68**: 65–67. <https://doi.org/10.1212/01.wnl.0000250258.76706.98>
93. Caldemeyer KS, Carrico JB, Mathews VP. The radiology and embryology of anomalous arteries of the head and neck. *AJR Am J Roentgenol* 1998; **170**: 197–203. <https://doi.org/10.2214/ajr.170.1.9423632>
94. Luh GY, Dean BL, Tomsick TA, Wallace RC. The persistent fetal carotid-vertebrobasilar anastomoses. *AJR Am J Roentgenol* 1999; **172**: 1427–32. <https://doi.org/10.2214/ajr.172.5.10227532>
95. Tubbs RS, Verma K, Riech S, Mortazavi MM, Shoja MM, Loukas M, et al. Persistent fetal intracranial arteries: A comprehensive review of anatomical and clinical significance. *J Neurosurg* 2011; **114**: 1127–34. <https://doi.org/10.3171/2010.11.JNS101527>
96. Sanders WP, Sorek PA, Mehta BA. Fenestration of intracranial arteries with special attention to associated aneurysms and other anomalies. *AJNR Am J Neuroradiol* 1993; **14**: 675–80.
97. Ballesteros-Acuña L, Gómez-Torres F, Estupiñán HY. Morphologic characterization of the superior cerebellar artery. A direct anatomic study. *Translational Research in Anatomy* 2021; **25**: 100150. <https://doi.org/10.1016/j.tria.2021.100150>
98. Perlmutter D, Rhoton AL. Microsurgical anatomy of the anterior cerebral-anterior communicating-recurrent artery complex. *J Neurosurg* 1976; **45**: 259–72. <https://doi.org/10.3171/jns.1976.45.3.0259>